Title

The pharmacokinetics of Zr-89 labeled liposomes over extended periods in a murine tumor model

Journal

Nuclear Medicine and Biology, 42(2)

ISSN

0969-8051

Authors

Seo, Jai Woong
Mahakian, Lisa M
Tam, Sarah
et al.

Publication Date

2015-02-01

DOI

10.1016/j.nucmedbio.2014.09.001

Peer reviewed

Published in final edited form as:
Nucl Med Biol. 2015 February ; 42(2): 155–163. doi:10.1016/j.nucmedbio.2014.09.001.

The pharmacokinetics of Zr-89 labeled liposomes over extended periods in a murine tumor model

Jai Woong Seo[*,a], **Lisa M. Mahakian**[a], **Sarah Tam**[a], **Shengping Qin**[a], **Elizabeth S. Ingham**[a], **Claude F. Meares**[b], and **Katherine W. Ferrara**[*,a]

[a] Department of Biomedical Engineering, University of California, Davis, CA 95616, USA

[b] Department of Chemistry, University of California, Davis, CA 95616, USA

Abstract

^{89}Zr ($t_{1/2}$ = 78.4 h), a positron-emitting metal, has been exploited for PET studies of antibodies because of its relatively long decay time and facile labeling procedures. Here, we used ^{89}Zr to evaluate the pharmacokinetics of long-circulating liposomes over 168 hours (1 week). We first developed a liposomal-labeling method using *p*-isothiocyanatobenzyldesferrioxamine (df-Bz-NCS) and df-PEG1k-DSPE. Df-Bz-NCS was conjugated to 1 mol% amino- and amino-PEG2k-DSPE, where the 1 mol% df-PEG1k-DSPE was incorporated when the liposomes were formulated. Incubation of ^{89}Zr with df, df-PEG1k, and df-PEG2k liposomes for one hour resulted in greater than 68% decay-corrected yield. The loss of the ^{89}Zr label from liposomes after incubation in 50% human serum for 48 hours ranged from ~1 to 3% across the three formulations. Tail vein administration of the three liposomal formulations in NDL tumor-bearing mice showed that the ^{89}Zr label at the end of the PEG2k brush was retained in the tumor, liver, spleen and whole body for a longer time interval than ^{89}Zr labels located under the PEG2k brush. The blood clearance rate of all three liposomal formulations was similar. Overall, the results indicate that the location of the ^{89}Zr label altered the clearance rate of intracellularly-trapped radioactivity and that df-PEG1k-DSPE provides a stable chelation site for liposomal or lipid-based particle studies over extended periods of time.

Keywords

liposomes; Zr-89; positron emission tomography; deferoxamine

[*]To whom correspondence should be addressed: Dr. Jai Woong Seo and Prof. Katherine W. Ferrara Dept. of Biomedical Engineering 451 Health Sciences Drive University of California, Davis Davis, CA 95616 PHONE 530-754-9436 (Prof. Ferrara), 530-304-0010 (Dr. Seo) FAX (530) 752 7156 kwferrara@ucdavis.edu.

Introduction

Liposomes, 100 nm size drug-delivery vehicles, have been used for more than four decades because of their biological compatibility and their stable blood circulation. Accumulation in leaky vasculature due to the enhanced permeability and retention (EPR) effect has been widely documented [1-5]. Radiometric quantitation has provided accurate pharmacokinetic profiling of liposomes *in vivo* [6]. Image-based quantitation of liposomes generated by single photon emission computed tomography (SPECT) or positron emission tomography (PET) also enables non-invasive data analysis over time [7-9]. Although radioisotopes for SPECT such as ^{67}Ga [10, 11], ^{111}In [12] and ^{99m}Tc [7, 13, 14] were exploited for early liposomal studies, due to the lower sensitivity of SPECT, PET using ^{18}F [8, 9], ^{68}Ga [15] and ^{64}Cu, [16-21] has now become a more attractive tool for liposomal pharmacokinetic studies.

For liposomal labeling, the radioactivity is sequestered in the hydrophilic interior cavity, in the lipid bilayer or on the surface of the liposome. Entrapment of radio metals with a chelator in the hydrophilic interior cavity [11, 14] or insertion of the radiolabeled lipid in the bilayer [8, 9] can require an elevated temperature, which may change liposomal properties. Surface radiolabeling of liposomes can be easily achieved at ambient temperature but the stability of the incorporated radioisotope must be evaluated. Since the half-life of ^{64}Cu (12.7 h) is suitable for evaluating liposomal kinetics for 48 hours and the blood half-life of liposomes is typically less than 48 hours, our laboratory has developed liposomal-labeling methods to chelate ^{64}Cu on the surface of stealth liposomes [16]. In previous studies, the stability of the ^{64}Cu-chelator and the ^{64}Cu-labeled lipid in liposomes was successfully evaluated over 48 hours *in vitro* and *in vivo* and several applications were reported [16-18].

Over the past decade, ^{89}Zr has emerged as a promising radioisotope for the labeling of molecules such as monoclonal antibodies (mAbs) or albumin, which have circulating half-lives from several days to a week [22-25]. ^{89}Zr has a lower fraction of gamma radiation than ^{124}I and ^{86}Y and therefore is preferable for PET imaging [26, 27]. In addition, ^{124}I ($t_{1/2}$ = 100 h), with a half-life comparable to ^{89}Zr, has been used to label mAb; however, the rapid clearance of ^{124}I from target cells due to enzymatic degradation of the labeled ^{124}I limits the target signal-to-noise ratio [28]. In contrast, metabolized ^{89}Zr remains within the tumor, liver, kidney and spleen and results in higher uptake in those tissues [28]. Deferoxamine (desferrioxamine (Df) B or desferal) has been used as a ^{89}Zr chelator with high binding affinity [29]. A series of deferoxamine bifunctional reagents such as *N*-(*S*-acetyl)thioacetyl-deferoxamine (SATA-df) [30], tetrafluorophenyl-*N*-succinyldesferal (TFA-*N*-SucDf) [31], and *p*-isothiocyanatobenzyl-desferoxaimine (df-Bz-NCS) [22, 23] has been developed for mAb conjugation (Figure 1). The stability of these reagents conjugated to mAbs has been evaluated previously and shown to be reliable for pharmacokinetic studies [22, 24, 30, 31].

Ideally, chemotherapeutic-laden liposomes should be internalized by tumor cells and result in tumor cell death, with the resulting cell debris cleared by macrophages through lymphatic channels. Alternatively, liposomes lacking cytotoxic activity can be trapped in tumor cell lysosomes [26, 28, 31]. In this context, we set out to track the fate of liposomes over extended periods of time using a radiolabeling strategy that should be superior to ^{124}I. We prepared three formulations of ^{89}Zr-labeled liposomes, with labels located on the surface, between the

surface and PEG2k tip and at the end of PEG2k brush. The stability of ^{89}Zr-labeled liposomes and the pharmacokinetic profile of these liposomes *in vivo* were evaluated in NDL (*neu* deletion) tumor-bearing mice [32, 33]. ^{89}Zr-images and biodistribution were acquired at 48 hours (2 days) and 168 hours (7 days) after systemic injection.

Materials and Methods

Lipids, DSPE-PEG2k-amine (1,2-distearoyl-*sn*-glycero-3-phosphoethanolamine-*N*-[amino(polyethylene glycol)-2000]), DSPE-amine (1,2-distearoyl-*sn*-glycero-3-phosphoethanolamine), HSPC (L-α-phosphatidylcholine, hydrogenated (Soy)), cholesterol, DSPE-PEG2k-OMe (1,2-distearoyl-*sn*-glycero-3-phosphoethanolamine-*N*-[methoxy(polyethylene glycol)-2000]), and DSPE-maleimide (1,2-distearoyl-*sn*-glycero-3-phosphoethanolamine-*N*-maleimide) were purchased from Avanti Polar Lipids (Alabaster, AL). Deferoxamine mesylate salt was purchased from Aldrich (St. Louis, MO). SPDP-dPEG®$_{16}$-NHS ester (SPDP-PEG1k-NHS) was purchased from Quanta BioDesign (Powell, OH). *p*-Isothiocyanatobenzyl-desferrioxamine was purchased from Macrocyclics (Dallas, TX). Solvents for the purification and isolation of product were purchased from EMD (Philadelphia, PA). Gels (Sephacryl-300 HR and Sephadex-G75 superfine) for the size-exclusion columns were purchased from GE Healthcare (Piscataway, NJ). Mouse serum was purchased from Innovative research (Novi, MI). ^{89}Zr was obtained from IBA (IBA Pharma, Belgium). All animal studies were conducted under a protocol approved by the University of California, Davis, Animal Care and Use Committee. MALDI mass spectrometry was performed using an ABI-4700 TOFTOF (Applied Biosystems, CA) with sinapinic acid matrix. Liposomal size distribution was measured by a Nicomp 380ZLS Particle Sizer (Particle Sizing Systems, CA).

Synthesis of df-PEG1k-SPDP (1)

As shown in Scheme 1, df-PEG1k-DSPE was synthesized in two steps from commercially-available deferoxamine (also known as desferrioxamine or desferal) and DSPE-amine (1,2-distearoyl-*sn*-glycero-3-phosphoethanolamine). Deferoxamine (df) mesylate (20 mg, 30 μmol) was dissolved in anhydrous DMSO in a 4 mL conical vial. SPDP-PEG1k-NHS (33 mg, 30 μmol) in anhydrous DMSO (1 mL) was added to the deferoxamine solution at room temperature; diisopropylethylamine (3.9 mg, 30 μmol) was then added. The solution was stirred for 4 hours at room temperature and the reaction was monitored by HPLC. The reaction mixture was poured into deionized water. Df-PEG1k-SPDP (36 mg, 65%) was isolated by HPLC (C12 column of 250 × 10 mm in size). Solvent A was 0.05% TFA in deionized water and solvent B was 0.05% TFA in acetonitrile. The flow rate was 3.0 mL/min; the gradient from 10-60% B occurred in 30 min, and the retention time was 22.7 min. MALDI analysis (reflector positive mode) showed a molecular mass peak at 1555.8 ($M + Na^+$, calculated 1555.8, see supporting information Fig. (SI-1) for mass spectrum).

Synthesis of df-PEG1k-DSPE (2)

DSPE-maleimide (16 μmol, 15 mg) in chloroform was placed in a thoroughly washed and dried test tube and the solvent was evaporated with nitrogen under a warm bath (50 °C). The resultant thin-lipid film was lyophilized for 4 hours in a test tube. Dried DSPE-maleimide

was suspended in degassed double-distilled water (0.5 mL) and sonicated repeatedly at 50 °C until the solution became transparent. The solution was then cooled to room temperature. Df-PEG1k-SPDP (30 μmol, 46 mg) was dissolved in double-distilled water and the pH was adjusted to 7.0 – 7.3 with 1 M NaOH. Tris(2-carboxyethyl)phosphine (0.1 M TCEP, pH 7, 1 mL) was added to the df-PEG1k-SPDP solution and incubated at room temperature for 10 min. Both solutions, df-PEG1k-SPDP and DSPE-maleimide, were combined and the pH was readjusted to 7.0 – 7.3. After 4 hours of incubation at room temperature, the reaction mixture was acidified to pH 2–3. Df-PEG1k-DSPE was isolated by HPLC (C4 column of 250 × 10 mm in size with solvents as above). The flow rate was 3.0 mL/min; the gradient from 50-90% B occurred in 40 min, and the retention time was 35 min. MALDI analysis (reflector positive mode) showed a molecular mass peak at 2346.6 ($M + Na^+$, calculated 2345.4, see Fig. SI-1 for mass spectrum).

Preparation of df-PEG1k liposomes

The liposomal-labeling method using df-PEG1k-DSPE is described in Figure SI-7 (middle column). For the df-PEG1k liposomes, the dried thin-lipid films with df-PEG1k-DSPE (total 10 mg lipids, see Table 1 for the formulation of liposomes) were suspended in 0.9% saline (0.5 mL, pH 7) and the solution was incubated for 5 – 10 min at 60 °C. The lipid mixture was extruded 21 times through a 100 nm membrane filter (Whatman® filter, NJ) unit on a heating block (60 – 62 °C). The df-PEG1k liposomal solution (20 mg/mL) was then stored at 4 °C for ^{89}Zr labeling.

Preparation of NH_2- and NH_2-PEG2k liposomes

NH_2-liposomes—The liposomal-labeling method using df-Bz-NCS is described in the left and right columns of Figure SI-7. In brief, lipids (total 10 mg) with DSPE-NH_2 (0.140 μmol) in chloroform (see Table 1 for the formulation of liposomes) were added to glass test tubes, which were thoroughly washed with chloroform. The solvent was evaporated with vortexing under gentle nitrogen flow after one minute of incubation in a warm water bath. The lipids were further dried in a lyophilizer for at least 4 hours. For the conjugation of df-Bz-NCS to NH_2-liposomes, the dried thin-lipid films were suspended in a saline (0.4 mL, pH 7.0) solution and incubated for 5 – 10 min at 60 °C. The lipid mixture was extruded 21 times through a 100 nm membrane filter (Whatman, NJ) unit on a heating block (60 – 62 °C). After cooling the lipid solution, excess df-Bz-NCS (0.6 mg, 0.77 μmol) dissolved in DMSO (15 μL) was added to the NH_2-liposomes (DSPE-NH_2 = 0.35 mM and df-Bz-NCS = 1.9 mM). The pH of the solution was adjusted to 8.5 by adding 0.15 M $NaHCO_3$ (pH 9.3) and both solutions were then incubated in a shaker (600 rpm) at 37 °C for 40 min. Df-NCS-conjugated liposomes were isolated by a size-exclusion column activated with 0.9% saline (300 mOsm). The size-exclusion column was packed as 1 cm in inner diameter and 7 cm in height. The liposomal fraction was collected in 2 mL and concentrated to a 20 mg/mL solution by an Amicon Ultra centrifugal filter (MWCO 100k, EMD Millipore, Billerica, MA) under 3000 RCF. Df liposomes in saline were stored at 4 °C for ^{89}Zr labeling. Df-Bz-NCS conjugation efficacy was measured by a fluorescamine assay[34]. The size of the liposomes was measured before and after df-Bz-NCS conjugation and after size-exclusion chromatography (Table 1). The lipid concentration was determined with a Phospholipids C assay (SI-2) to be 64% of the initial mass of lipid on average.

NH_2-PEG2k liposomes—The preparation followed the procedure above with DSPE-PEG2k-amine substituted for DSPE-NH_2.

General procedure for preparation of ^{89}Zr-labeled liposomes

^{89}Zr(IV) oxalate (63.9 MBq, 50 μL) in 1 M oxalic acid was mixed with a 2 M Na_2CO_3 (23 μL) solution and incubated at room temperature for 5 min. 0.5 M HEPES buffer (0.25 ml, pH 7.0) was added and was further diluted with double distilled water (0.2 mL). Df-conjugated liposomes in 0.9% saline (2 mg, 0.11 mL) were added to the ^{89}Zr solution and the final volume of the solution was 0.633 ml. The mixture was incubated at room temperature for 1 hour. To remove free ^{89}Zr, 0.1 M EDTA (20 μL) was added to the liposomal mixture and ^{89}Zr-labeled liposomes were immediately isolated with a size-exclusion column (Sephadex G-75, GE Healthcare) preequilibrated with 0.9% saline (pH 7). Under the same reaction conditions, NH_2 and NH_2-PEG2k liposomes were also evaluated to provide a basis for comparison of the resulting liposomal labeling. Isolated liposomal fractions were combined and concentrated by Amicon Ultra filter (MWCO, 100k) with centrifugation (30 min, 4000 rpm) to less than 300 μL. Freshly prepared ^{89}Zr-labeled liposomes were immediately used in *in vitro* and *in vivo* studies.

In vitro stability in human serum

^{89}Zr-labeled liposomes (0.67 ± 0.064 MBq (n = 3), 1 mg, 50 μL) in saline were added to human serum (0.5 mL) and diluted with saline (pH 7, 0.45 mL) to produce 50% serum. The stability of ^{89}Zr-labled liposomes was evaluated in 50% serum as in previously-reported liposomal studies [13, 14, 16]. Dilution of serum for such studies is typically performed to approximate the components of various proteins in blood. The ^{89}Zr-liposome serum mixture was incubated at 37 °C for 48 hours at a pH of 7. The serum mixture (100 μL) was drawn at 48 hours and isolated via a size-exclusion column (Sephacryl-300 HR, height: 300 mm, ID: 10 mm) with PBS (pH 7) as a mobile phase. Radioactivity and absorbance (280 nm) were measured by a radio- (Bioscan INC, NW) and UV- detector connected to the HPLC (Thermoscientific, Dionex UltimMate 3000). Liposomal stability was also evaluated with instant thin layer chromatography (ITLC, Biodex, NY). Liposomal serum mixtures (1 μL) were spotted on the ITLC and eluted with 0.1 M ammonium citrate (pH 5.5). Radioactivity was detected by a radioTLC scanner (Bioscan, NW).

NDL tumor transplantation

Each 5 to 6-week-old FVB mouse was anesthetized by an IP injection of a Ketamine/Xylazine mixture (50 – 100 mg/kg Ketamine: 5 mg/kg Xylazine). Once anesthetized, the animal was placed under a warming lamp, shaved with clippers and the surgical site was disinfected. Tumors from NDL mice (an ErbB-2/neu-overexpressing mouse mammary tumor) were processed into one cubic-millimeter-sized pieces for transplantation [32, 33, 35]. Once the recipient animal was prepared for surgery and deeply anesthetized, a 0.5 cm incision was made adjacent to the #4 mammary nipples on the right and left sides and a one cubic-millimeter piece of donor tumor was transplanted into the 4th inguinal mammary fat pads of the recipient mouse. The surgical site was closed with one wound clip per side, and a one-time injection of Buprenex or equivalent was given at 0.05 – 0.1 mg/kg before the

animal was ambulatory. The wounds were monitored for seven days at which point the wound clips were removed. Approximately 3 weeks post surgery, mice with palpated bilateral tumors of < 1 cc were included in this study.

PET Scans, Time-Activity Curves (TAC) and biodistribution

Mice were anesthetized with 3.0% isoflurane in oxygen and maintained under 1.5 – 2.0% isoflurane. ^{89}Zr-labeled liposomes for PET and 168-hour biodistribution (0.53 ± 0.05 mg/animal, 12.1 ± 1.0 MBq/animal, n = 14) were administered via tail vein injection, and PET images were acquired at 0, 24, 48, 72, 120 and 168 hours followed by biodistribution analysis at 168 hours. For the 48-hour biodistribution analysis, a similar amount of ^{89}Zr-labeled liposomes (0.25 ± 0.01 mg/animal, 1.8 ± 0.2 MBq/animal, n = 9) in PBS (pH 7.0, 150 μL/animal) was injected. PET imaging of ^{89}Zr-labeled liposomes was conducted with the microPET-Focus 120 (Concorde Microsystems, Inc., TN) for 30 min at 0, 24, 48, 72, 120 and 168 hours post injection. Maximum a posteriori (MAP) reconstruction was performed with ASIPro software (CTI Molecular Imaging). TACs of blood, liver and spleen were obtained by region-of interest (ROI) analysis using ASIPro software and represented as the percentage of injected dose per cubic centimeter (%ID/cc). Whole body activity was measured with a gamma-counter (Capintec, Inc. NJ) and normalized by the initial value. The mice were euthanized with an IV injection of Euthasol (Western Medical Supply, CA), and the blood was perfused from the body with Dulbecco's Modified Eagle Medium (DMEM, Invitrogen, CA). Organs and bodily fluids, including blood, urine, heart, lungs, liver, spleen, kidneys, muscle, bone, colon, small intestines and tumors, were harvested. Organ weights were measured with a microbalance after washing with PBS and removing residual water. Radioactivity was measured using a 1470 automatic gamma counter (PerkinElmer, CT). Radioactive accumulation was presented as the %ID per gram of tissue (%ID/g). All TAC and biodistribution data were decay-corrected.

Pharmacokinetic model

A previously-developed pharmacokinetic model for radio-labeled liposomes was used to calculate liposomal pharmacokinetic parameters [17, 36]. Clearance curves of the three liposomal formulations were generated based on a modified version of a previously-developed model [17, 36]. Considering the negligible effects of the tissue compartment on the permeability prediction for the long-circulating liposomes, the tissue compartment has been eliminated in the calculation applied here. The liposomal half-life in the blood pool was estimated using a one-phase exponential decay model $C_B = C_0 e^{-kt}$ by Prism (GraphPad Software, CA). The average weight was 21.73 g for mice injected with ^{89}Zr-df liposomes, 22.06 g for ^{89}Zr-df-PEG1k liposomes, and 21.94 g for ^{89}Zr-df-PEG2k liposomes. The blood volume density was set to be 0.9 g/mL. The volume of distribution (VD) of liposomes was assumed to be equal to the total blood volume. Based on the measured radioactivity data in blood and mouse whole body, the elimination rate was calculated by:

$$k_e = \frac{1}{V_B} \frac{100 - wC_b(T)}{\int_0^T C_B dt}$$

where w is the mouse average weight (g), V_B is the volume of distribution of liposomes in the blood (mL), C_B is the average radioactivity per unit volume in blood (ID%/cc), C_b is the average whole-body radioactivity per unit gram (ID%/g) and T is the measured time period (hr). The clearance of the radioactivity (CL) was obtained by $k_e V_B$ (mL/hr).

Statistical analysis

Each time-activity curve (TAC) was fit by a single-phase decay curve. Curve fits were compared with an extra sum-of-squares F test. Comparison of the liposomal formulations was performed with two-way ANOVA followed by Tukey's test for multiple comparisons (SI-6).

Results

Synthesis of Df-PEG1k-DSPE

In order to label ^{89}Zr within a 5 mol% PEG2k-OMe brush (Figure SI-7), df-PEG1k-DSPE was synthesized from deferoxamine in two steps (Scheme 1). One equivalent of SPDP-PEG1k-NHS afforded a 65% yield of the df-PEG1k-SPDP (**1**). The resulting df-PEG1k-SPDP was further conjugated to DSPE-maleimide. Due to the low solubility of lipophilic DSPE-maleimide, DSPE-maleimide micelles were self-assembled before conjugation with df-PEG1k-SPDP. After the activation of two equivalents of df-PEG1k-SPDP with a 5-fold molar excess of TCEP, which affords a free thiol, the reaction of activated df-PEG1k-SPDP with DSPE-maleimide micelles was completed within 4 hours at room temperature. HPLC purification gave more than 95% purity of df-PEG1k-DSPE.

^{89}Zr labeling on liposomes

Df liposomes and df-PEG2k liposomes were prepared by thiourea formation from NH_2 and NH_2-PEG2k liposomes as shown in Figure SI-7, and their lipid components are shown in Table 1. First, df-Bz-NCS (5.5 equiv per liposomal amine) was coupled to the amine group on liposomes at pH 8.5. Size-exclusion column chromatography (Sepadex-G75, GE Healthcare) in 0.9% saline solution removed excess unreacted df-Bz-NCS and other small molecules. A fluorescamine assay[34] showed the presence of 15.3 ± 2.7% (n = 6) of unreacted amine, which may result from NH_2-DSPE or NH_2-PEG2k-DSPE on the inner leaflet. In the case of df-PEG1k liposomes, liposomes were formulated with 1 mol% df-PEG1k-DSPE in 0.9% saline solution, and the crude liposomal solution was used directly for ^{89}Zr labeling (Figure SI-7).

^{89}Zr in 1 M oxalic acid solution was diluted and buffered to create an isotonic solution (pH 7) as described in the Methods section. With this ^{89}Zr oxalate cocktail solution, the labeling of ^{89}Zr with df, df-PEG1k, and df-PEG2k liposomes was performed in 0.9% saline (pH 7). Liposomes, isolated with a size-exclusion column (0.9% NaCl, pH 7), retained a pH of 7 after separation. The overall decay-corrected labeling yield was greater than 68% (df liposomes: 68 ± 24% (n = 9), df-PEG1k liposomes: 77 ± 6.7% (n = 6), df-PEG2k liposomes: 75 ± 17% (n = 9)) and the radiochemical purity of ^{89}Zr-labeled liposomes on reverse-phase TLC was greater than 95%. Under the same reaction conditions, radioactivity was not detected in the liposomal fraction for NH_2 and NH_2-PEG2k liposomes incubated with

the ^{89}Zr oxalate cocktail solution. The specific activity of the liposomes calculated by a phospholipid assay was greater than 36.5 ± 3.0 MBq/mg (37.2 ± 3.0 MBq/μmol lipid)

In vitro stability of ^{89}Zr-labeled liposomes

We evaluated the serum stability of ^{89}Zr-labeled liposome for an interval of up to 48 hours, as more than 90% of the radioactivity associated with liposomes is cleared from the blood pool within this period *in vivo*. ^{89}Zr-labeled df, df-PEG1k and df-PEG2k liposomes were incubated at 37 °C in a 50% human serum solution prepared with 0.9% saline at pH 7. At 24 and 48 hours after incubation, the serum solution with ^{89}Zr-labeled liposomes was loaded into a size-exclusion column (Sephacryl-300HR) to determine the radioactivity associated with the liposomes or serum proteins (Figure 2). The pH of the solution was maintained at 7 for 48 hours in all cases. The retention time of liposomes detected at 280 nm was 9 minutes (Figure 2a, dotted line), whereas that of the serum proteins was 14 minutes (Figure 2a, solid line). Radiochromatograms from serum solutions incubated with ^{89}Zr-df (Figure 2b), ^{89}Zr-df-PEG1k (Figure 2c), and ^{89}Zr-df-PEG2k liposomes (Figure 2d) showed that the integration of liposomal peaks (7 – 11 min) was greater than 96% and that of serum proteins (12 – 16 min) was less than 4%. ITLC was also performed to evaluate the dissociated ^{89}Zr from liposomes. The retention factor (Rf) of ^{89}Zr incubated with serum (SI-3, b) and free ^{89}Zr (SI-3, a) was > 0.9 whereas that of ^{89}Zr associated with liposomes (SI-3, c-f) was < 0.1. For the three formulations of liposomes, 97 – 99% of the radioactive label detected at 0 hours remained present at the 48-hour time point (Table 2). Size-exclusion chromatography and ITLC both validated the stability of ^{89}Zr labels on liposomes.

Image-based pharmacokinetic study of liposomes

Analysis of manually-drawn 3-dimensional ROIs from images of the tumors, liver and spleen obtained at 0.5, 24, 48, 72, 128, and 168 hours demonstrates the differences in accumulation and clearance of these liposomal formulations (Figure 3 and Figure 4). Blood activity was measured by drawing an ROI on the left ventricle of the heart. Figure 4a shows the clearance of ^{89}Zr-labeled liposomes from blood. The half-life of ^{89}Zr-df, ^{89}Zr-df-PEG1k, ^{89}Zr-df-PEG2k liposomes, calculated from a one-phase exponential decay model, was 13.3, 15.9, and 12.8 hours, respectively. After 48 hours, the blood radioactivity was less than 5% ID/cc.

Over 168 hours, the accumulation of ^{89}Zr-df-PEG2k liposomes in NDL tumors was significantly greater than ^{89}Zr-df liposomes (n=7~10, $p < 0.0001$), although the major difference in accumulation resulted from the increased concentration at the later time points. The peak accumulation of ^{89}Zr-df-PEG2k liposomes (occurring at 48 hours) was 7.7 ± 1.9 %ID/cc (n=5) and that of ^{89}Zr-df and ^{89}Zr-df-PEG1k liposomes (occurring at 24 hours) was 6.3 ± 1.2 %ID/cc (n=4) and 7.8 ± 1.0 %ID/cc (n=5), respectively. Accumulated radioactivity from ^{89}Zr-df-PEG2k liposomes also remained in tumors for a longer period of time as compared with ^{89}Zr-df and ^{89}Zr-PEG1k liposomes (Figure 4b).

We also investigated radioactive accumulation in the liver and spleen over 168 hours. At 24 hours after injection, the accumulation of ^{89}Zr-df-PEG2k liposomes in the spleen (12.8 ± 1.2 %ID/cc) and liver (15 ± 2.6 %ID/cc) was not significantly higher than ^{89}Zr-df (spleen: 10.5

± 1.5 %ID/cc, liver: 14.2 ± 0.6 %ID/cc) and ^{89}Zr-df-PEG1k liposomes (spleen: 9.1 ± 0.7 %ID/cc, liver: 13.3 ± 1.3 %ID/cc) (Figure 4c,d, SI-6). At 48 hours after injection, radioactivity in the liver ($p<0.0001$) and spleen ($p<0.001$) resulting from the injection of ^{89}Zr-df-PEG2k liposomes was significantly higher than that resulting from other liposomes. Whole-body PET images showed that the clearance of radioactivity from liposomes was primarily through the liver and spleen (Figure 3).

Pharmacokinetic parameters were calculated based on previously developed methods (Table 3) [17]. The whole body clearance (CL) of ^{89}Zr-df-PEG2k liposomes (0.053 mL/h) was slower than ^{89}Zr-df- (0.085 mL/h, $p<0.0001$) and ^{89}Zr-df-PEG1k liposomes (0.077 mL/h, $p<0.0001$). Alternatively, the blood half-life of the three liposomes was 13.3 h (^{89}Zr-df liposomes), 15.9 h (^{89}Zr-df-PEG1k liposomes), and 12.8 h (^{89}Zr-df-PEG2k liposomes), which were not significantly different. The whole-body clearance was not correlated with the clearance of the liposomes from the blood pool (Figure 4a, e).

Biodistribution

The average %ID/g of blood, urine, heart, lungs, liver, spleen, kidney, muscle, bone, colon, small intestines and tumors is presented in Table 4. Between 48 hours and 168 hours after injection, radioactivity in most organs decreased or remained constant. However, the radioactive concentration in the spleen increased at the later time point (168 hours) as compared with the earlier time point. This enhanced concentration of radioactivity appeared to result from a decrease in the weight of the spleen over the course of the study (210 ± 32 mg, n=6, at 48 hours, 81 ± 15 mg, n=6, at 168 hours, *t*-test: $p<0.0001$).

At 48 hours after administration, the radioactivity in all lymph nodes was < 8% ID/g (Figure 5a); however, at 168 hours, the nodal radioactivity varied, with several lymph nodes (# 8, 11, 13 and 14) in mice injected with ^{89}Zr-df-PEG2k liposomes demonstrating accumulation that was greater than 15 %ID/g (Figure 5b). This enhanced uptake within these nodes was further evaluated with immunohistochemistry to determine whether metastatic tumors could be detected. However, Cytokeratin 8 and 18 (CK8/18) staining was similar for nodes with high and low levels of accumulated radioactivity (Fig. SI-5).

Discussion

In previous studies, the labeling of antibodies with ^{89}Zr has been efficiently accomplished with high specific activity using deferoxamine.[37-39] Since monoclonal antibodies (mAbs) can circulate for several weeks, the 78.4-hour half-life of ^{89}Zr positron decay is useful in such studies. Likewise, labeling of long-circulating liposomes or other nanoparticles with ^{89}Zr can facilitate pharmacokinetic studies that extend over 1-2 weeks.

Meijs *et al.* initially introduced ^{89}Zr labeling with desferal linked on a resin [29]. In this work, reacti-gel with imidazoyl carbamate groups was employed to couple desferal in order to evaluate the stability of the ^{89}Zr-df complex conjugates. For ^{89}Zr conjugation to mAbs, *S*-acetylthioacetate-desferal (SATA-df) has been previously used as a bifunctional chelator [29, 30]. Later, Verel *et al.* synthesized an activated tetrafluorophenyl-*N*-succinyldf (TFP-*N*-sucDf) ester, which was reacted with amines on the mAb via amide formation [31]. *p*-

Isothicyanatobenzyl desferrioxamine (df-Bz-NCS), which forms a thiourea, was also introduced for facile radiolabeling of mAbs [22, 23]. Most recently, Tinianow *et al.* developed a specific conjugation of bifunctional chelators such as maleimidocyclohexyl-desferrioxamine (df-Chx-Mal), bromoacetyldesferrioxamine (df-Bac) and iodoacetyl-desferrioxamine (df-lac) to the thiol on mAbs (Figure 1) [24]. However, ^{89}Zr has rarely been applied for nanoparticle studies until now[40, 41].

In an analogous approach, here we conjugated df-Bz-NCS to an amine on the liposomal surface. Commercially available DSPE-NH_2 and DSPE-PEG2k-NH_2 were introduced into the liposome bilayer (Table 1), and those amine groups (1 mol% relative to total lipids) were conjugated with df-Bz-NCS (Figure SI-7, left and right column). Conjugation of df-Bz-NCS to the free amine followed a conventional conjugation protocol that maintains the solution at > pH 8.5 [22]. The 85% conjugation yield of df-Bz-NCS (12 nmol deferoxamine/mg lipid, 0.24 mM deferoxamine), measured by a fluorescamine assay, was sufficient to incorporate ^{89}Zr (> 18 MBq/nmol) with high specific activity. Meijs *et al.* and Perk *et al.* measured the rate of ^{89}Zr complexation with different buffers and pH values [22, 29]. Those reports demonstrated that maintaining the pH between 6.8 and 7.2 is the optimal condition for complexation within one hour. In our liposomal labeling system, ^{89}Zr complexation in isotonic conditions was required to preserve liposomal stability. To satisfy all conditions, we optimized the conditions to use a 1:0.46:5:4 (1 M oxalate ^{89}Zr solution: 2 M Na_2CO_3: 0.5 M HEPES : double-distilled water, v:v:v:v) ratio cocktail, which results in an isotonic condition (osmolality: ~ 300 mOsm) and an optimal pH at 7. This cocktail resulted in a decay-corrected yield greater than 70%.

The *in vitro* stability of the ^{89}Zr label on deferoxamine-monoclonal antibodies (df-mAbs) measured in serum [31] previously showed less than 4% dissociation of radioactivity over 48 hours[22, 24, 28]. Similarly, we evaluated the stability of three liposomal formulations: ^{89}Zr-df, ^{89}Zr-df-PEG1k, and ^{89}Zr-df-PEG2k liposomes, which have ^{89}Zr-df labels at three different locations (Figure SI-7) and different linkers such as thioether and thiourea. The ^{89}Zr-liposomal stability evaluated in 50% human serum with 0.9% saline at pH 7 over 48 hours showed a minimal loss of the ^{89}Zr label (< 3%) from liposomes (Table 2, Figure 2, Fig. SI-3). The location of the ^{89}Zr label and different linkers did not alter the stability of the label in human serum. The stability of ^{89}Zr-labeled liposomes was therefore sufficient to measure the pharmacokinetics of liposomes in an *in vivo* study.

The half-life of ^{89}Zr-df-labeled liposomes in the blood pool was 13 - 16 hours (Table 3), without a significant difference between the formulations. This result demonstrated that all ^{89}Zr-labeling methods tested here were sufficiently stable to enable ^{89}Zr-labeling for liposomal studies (Figure 4). However, we observed a significantly different accumulation at later time points (72, 120, and 168 hours (Table SI-6-2)) between ^{89}Zr-df-PEG2k liposomes as compared with ^{89}Zr-df and ^{89}Zr-df-PEG1k liposomes in tissues such as the liver, spleen and tumor (Figure 4). Interestingly, the splenic accumulation of ^{89}Zr-df-PEG2k liposomes obtained from ROI analysis (17.07 ± 2.67 %ID/cc at 168 hours) was different from that of the biodistribution (65.7 ± 24.4 %ID/g at 168 hours). The difference was found to be due to the decreased weight (2.6 fold) of the spleen at the time of biodistribution analysis (although the volume of the spleen from ROI analysis was similar over 168 hours). We hypothesize

that the relatively large amount of residual ^{89}Zr in the spleen may have altered the splenic biology. We are not aware of previous reports regarding splenic toxicity of ^{89}Zr; however, at this time, there are few studies with ^{89}Zr-labeled nanoparticles.

The retention time of radioactivity in tissues varied with the location of the ^{89}Zr label. The higher residual radioactivity in the spleen and liver with ^{89}Zr-df-PEG2k liposomes (Figure 4c, d) may indicate that ^{89}Zr labels at the end of the PEG brush are more easily dissociated from liposomes than ^{89}Zr labels under a 5 mol% PEG2k-brush. Intercellular protein interaction and dissociation of radiometals tend to increase the residual radiometal in cells [28]. Although several ^{89}Zr-df-mAbs with different short linkers have been tested for the residualization of radiometals[24, 31], the effect of a long PEG spacer between the ^{89}Zr-df label and carrier has not been reported.

The whole-body images (Figure 3) and biodistribution study (Table 4) demonstrated that the radioactivity was primarily cleared through the liver and spleen. The higher uptake in the colon, small intestine and urine at the later time points (48 and 168 hours (Table 4)) demonstrate that ^{89}Zr liposomes were processed through the hepatobiliary system. Verel *et al.* compared a chimeric monoclonal antibody, labeled with ^{89}Zr, ^{88}Y, ^{124}I, and ^{131}I, and demonstrated that the radioactivity of ^{89}Zr and ^{88}Y was trapped in tumors, liver and spleen to a greater extent than ^{124}I and ^{131}I [28].

The NDL tumor model is a syngeneic, orthotopic tumor, which can be implanted in mice with a fully-intact immune system. Additionally, it is a Her2+ tumor with similar biology to a subset of human breast cancer. Because of our interest in looking at lymphatics as well as the trafficking of macrophages, a syngeneic, orthotopic model was appropriate. As we have previously observed for ^{64}Cu-lipsosomal uptake in mouse mammary intraepithelial neoplasia outgrowth (MIN-Os) tumors [42] and MET-1 mammary carcinoma [43], the accumulation of ^{89}Zr liposomes was primarily concentrated in the peripheral region of the tumor, reflecting the angiogenic status of the tumor periphery.

Radiometals are likely to accumulate in tumors [26, 28, 31] and particularly in tumor macrophages[40]. We found that the radioactivity increased over time in a subset of lymph nodes to a maximum of 26 %ID/g at 168 hours after liposome injection (Figure 5). These results indicate that the high radioactivity in lymph nodes may be due to drainage of radioactive liposomes or metabolites or the transport of radioactivity to the lymph nodes by macrophages. In this small preliminary study, greater lymphatic accumulation was observed following the injection of ^{89}Zr-df-PEG2k liposomes and may result from the higher tumor accumulation at later time points or from greater uptake of the ^{89}Zr-df-PEG2k liposomes (with the exposed chelator) by tumor macrophages. The differences in lymphatic or macrophage uptake must be tested in future studies.

In conclusion, ^{89}Zr-df labeling of a liposomal system facilitated studies of liposome pharmacokinetics over a one-week time period. The time-activity curve within the blood pool was similar for liposomes with an exposed or buried radioisotope; however, whole-body clearance was reduced for the exposed radioisotope. In the future, long-circulating nanoparticles applied as drug-delivery systems will require ^{89}Zr as a probe for image-based

pharmacokinetics, and such studies will require optimization of the chelator and attachment strategy.

Supplementary Material

Refer to Web version on PubMed Central for supplementary material.

Acknowledgement

We thank the staff in the CMGI (Center for Molecular and Genomic Imaging, UC Davis) for assistance in the imaging study and Dr. William T. Jewell at CMSF (Campus Mass Spectrometry Facilities, UC Davis) for comments on mass analysis. We also thank Dr. Jason S. Lewis at Memorial Sloan-Kettering Cancer Center for providing ^{89}Zr. We appreciate the support of NIH R01CA134659 and R01CA103828.

References

1. Torchilin VP. Recent advances with liposomes as pharmaceutical carriers. Nat Rev Drug Discov. 2005; 4:145–160. [PubMed: 15688077]
2. Torchilin VP, Omelyanenko VG, Papisov MI, Bogdanov AA, Trubetskoy VS, Herron JN, Gentry CA. Poly(Ethylene Glycol) on the Liposome Surface - on the Mechanism of Polymer-Coated Liposome Longevity. Bba-Biomembranes. 1994; 1195:11–20. [PubMed: 7918551]
3. Klibanov AL, Maruyama K, Torchilin VP, Huang L. Amphipathic Polyethyleneglycols Effectively Prolong the Circulation Time of Liposomes. Febs Lett. 1990; 268:235–237. [PubMed: 2384160]
4. Gabizon A, Shmeeda H, Barenholz Y. Pharmacokinetics of pegylated liposomal doxorubicin - Review of animal and human studies. Clin Pharmacokinet. 2003; 42:419–436. [PubMed: 12739982]
5. Matsumura Y, Maeda H. A New Concept for Macromolecular Therapeutics in Cancer-Chemotherapy - Mechanism of Tumoritropic Accumulation of Proteins and the Antitumor Agent Smancs. Cancer Res. 1986; 46:6387–6392. [PubMed: 2946403]
6. Phillips WT, Goins BA, Bao A. Radioactive liposomes. Wires Nanomed Nanobi. 2009; 1:69–83.
7. Laverman P, Dams ETM, Oyen WJG, Storm G, Koenders EB, Prevost R, van der Meer JWM, Corstens FHM, Boerman OC. A novel method to label liposomes with Tc-99m by the hydrazino nicotinyl derivative. J Nucl Med. 1999; 40:192–197. [PubMed: 9935076]
8. Marik J, Tartis MS, Zhang H, Fung JY, Kheirolomoom A, Sutcliffe JL, Ferrara KW. Long-circulating liposomes radiolabeled with [F-18]fluorodipalmitin ([F-18]FDP). Nucl Med Biol. 2007; 34:165–171. [PubMed: 17307124]
9. Urakami T, Akai S, Katayama Y, Harada N, Tsukada H, Oku N. Novel amphiphilic probes for [F-18]-radiolabeling preformed liposomes and determination of liposomal trafficking by positron emission tomography. J Med Chem. 2007; 50:6454–6457. [PubMed: 18052025]
10. Gabizon A, Papahadjopoulos D. Liposome Formulations with Prolonged Circulation Time in Blood and Enhanced Uptake by Tumors. P Natl Acad Sci USA. 1988; 85:6949–6953.
11. Ogiharaumeda I, Kojima S. Increased Delivery of Ga-67 to Tumors Using Serum-Stable Liposomes. J Nucl Med. 1988; 29:516–523. [PubMed: 3351606]
12. Harrington KJ, Rowlinson-Busza G, Syrigos KN, Uster PS, Vile RG, Stewart JSW. Pegylated liposomes have potential as vehicles for intratumoral and subcutaneous drug delivery. Clin Cancer Res. 2000; 6:2528–2537. [PubMed: 10873109]
13. Phillips WT, Rudolph AS, Goins B, Timmons JH, Klipper R, Blumhardt R. A Simple Method for Producing a Tc-99m-Labeled Liposome Which Is Stable Invivo. Nucl Med Biol. 1992; 19:539–547.
14. Bao A, Goins B, Klipper R, Negrete G, Mahindaratne M, Phillips WT. A novel liposome radiolabeling method using Tc-99m-“SNS/S” complexes: In vitro and in vivo evaluation. J Pharm Sci. 2003; 92:1893–1904. [PubMed: 12950007]
15. Helbok A, Decristoforo C, Dobrozemsky G, Rangger C, Diederen E, Stark B, Prassl R, von Guggenberg E. Radiolabeling of lipid-based nanoparticles for diagnostics and therapeutic

applications: a comparison using different radiometals. J Liposome Res. 2010; 20:219–227. [PubMed: 19863193]

16. Seo JW, Zhang H, Kukis DL, Meares CF, Ferrara KW. A Novel Method to Label Preformed Liposomes with Cu-64 for Positron Emission Tomography (PET) Imaging. Bioconjugate Chem. 2008; 19:2577–2584.
17. Seo JW, Qin SP, Mahakian LM, Watson KD, Kheirolomoom A, Ferrara KW. Positron emission tomography imaging of the stability of Cu-64 labeled dipalmitoyl and distearoyl lipids in liposomes. J Control Release. 2011; 151:28–34. [PubMed: 21241753]
18. Seo JW, Mahakian LM, Kheirolomoom A, Zhang H, Meares CF, Ferdani R, Anderson CJ, Ferrara KW. Liposomal Cu-64 Labeling Method Using Bifunctional Chelators: Poly(ethylene glycol) Spacer and Chelator Effects. Bioconjugate Chem. 2010; 21:1206–1215.
19. Qin SP, Seo JW, Zhang H, Qi J, Curry FRE, Ferrara KW. An Imaging-Driven Model for Liposomal Stability and Circulation. Mol Pharm. 2010; 7:12–21. [PubMed: 19621944]
20. Petersen AL, Binderup T, Jolck RI, Rasmussen P, Henriksen JR, Pfeifer AK, Kjaer A, Andresen TL. Positron emission tomography evaluation of somatostatin receptor targeted Cu-64-TATE-liposomes in a human neuroendocrine carcinoma mouse model. J Control Release. 2012; 160:254–263. [PubMed: 22245688]
21. Petersen AL, Binderup T, Rasmussen P, Henriksen JR, Elema DR, Kjaer A, Andresen TL. Cu-64 loaded liposomes as positron emission tomography imaging agents. Biomaterials. 2011; 32:2334–2341. [PubMed: 21216003]
22. Perk LR, Vosjan MJWD, Visser GWM, Budde M, Jurek P, Kiefer GE, van Dongen GAMS. p-Isothiocyanatobenzyl-desferrioxamine: a new bifunctional chelate for facile radiolabeling of monoclonal antibodies with zirconium-89 for immuno-PET imaging. Eur J Nucl Med Mol I. 2010; 37:250–259.
23. Vosjan MJWD, Perk LR, Visser GWM, Budde M, Jurek P, Kiefer GE, van Dongen GAMS. Conjugation and radiolabeling of monoclonal antibodies with zirconium-89 for PET imaging using the bifunctional chelate p-isothiocyanatobenzyl desferrioxamine. Nat Protoc. 2010; 5:739–743. [PubMed: 20360768]
24. Tinianow JN, Gill HS, Ogasawara A, Flores JE, Vanderbilt AN, Luis E, Vandlen R, Darwish M, Junutula JR, Williams SP, Marik J. Site-specifically Zr-89 labeled monoclonal antibodies for ImmunoPET. Nucl Med Biol. 2010; 37:289–297. [PubMed: 20346868]
25. Heneweer C, Holland JP, Divilov V, Carlin S, Lewis JS. Magnitude of Enhanced Permeability and Retention Effect in Tumors with Different Phenotypes: Zr-89 Albumin as a Model System. J Nucl Med. 2011; 52:625–633. [PubMed: 21421727]
26. Perk LR, Visser GWM, Vosjan MJWD, Stigter-van Walsum M, Tijink BM, Leemans CR, van Dongen GAMS. Zr-89 as a PET surrogate radioisotope for scouting biodistribution of the therapeutic radiometals Y-90 and Lu-117 in tumor-bearing nude mice after coupling to the internalizing antibody cetuximab. J Nucl Med. 2005; 46:1898–1906. [PubMed: 16269605]
27. Lubberink M, Herzog H. Quantitative imaging of I-124 and Y-86 with PET. Eur J Nucl Med Mol I. 2011; 38:10–18.
28. Verel I, Visser GWM, Boerman OC, van Eerd JEM, Finn R, Boellaard R, Vosjan MJWD, Walsum MSV, Snow GB, van Dongen GAMS. Long-lived positron emitters zirconium-89 and iodine-124 for scouting of therapeutic radioimmunoconjugates with PET. Cancer Biother Radio. 2003; 18:655–661.
29. Meijs WE, Herscheid JDM, Haisma HJ, Pinedo HM. Evaluation of Desferal as a Bifunctional Chelating Agent for Labeling Antibodies with Zr-89. Appl Radiat Isotopes. 1992; 43:1443–1447.
30. Meijs WE, Haisma HJ, Klok RP, vanGog FB, Kievit E, Pinedo HM, Herscheid JDM. Zirconium-labeled monoclonal antibodies and their distribution in tumor-bearing nude mice. J Nucl Med. 1997; 38:112–118. [PubMed: 8998164]
31. Verel I, Visser GWM, Boellaard R, Stigter-van Walsum M, Snow GB, van Dongen GAMS. Zr-89 immuno-PET: Comprehensive procedures for the production of Zr-89-labeled monoclonal antibodies. J Nucl Med. 2003; 44:1271–1281. [PubMed: 12902418]

32. Miller JK, Shattuck DL, Ingalla EQ, Yen LL, Borowsky AD, Young LJT, Cardiff RD, Carraway KL, Sweeney C. Suppression of the Negative Regulator LRIG1 Contributes to ErbB2 Overexpression in Breast Cancer. Cancer Res. 2008; 68:8286–8294. [PubMed: 18922900]
33. Ingalla EQ, Miller JK, Wald JH, Workman HC, Kaur RP, Yen L, Fry WHD, Borowsky AD, Young LJT, Sweeney C, Carraway KL. Post-transcriptional Mechanisms Contribute to the Suppression of the ErbB3 Negative Regulator Protein Nrdp1 in Mammary Tumors. J Biol Chem. 2010; 285:28691–28697. [PubMed: 20628057]
34. Udenfrie S, Stein S, Bohlen P, Dairman W. Fluorescamine - Reagent for Assay of Amino-Acids, Peptides, Proteins, and Primary Amines in Picomole Range. Science. 1972; 178:871–872. [PubMed: 5085985]
35. Ursini-Siegel J, Schade B, Muller WJ, Cardiff RD. Timeline - Insights from transgenic mouse models of ERBB2-induced breast cancer. Nat Rev Cancer. 2007; 7:389–397. [PubMed: 17446858]
36. Qin S, Seo JW, Zhang H, Qi J, Curry F-RE, Ferrara KW. An Imaging-Driven Model for Liposomal Stability and Circulation. Molecular Pharmaceutics. 2009; 7:12–21. [PubMed: 19621944]
37. McCabe KE, Wu AM. Positive Progress in ImmunoPET-Not Just a Coincidence. Cancer Biother Radio. 2010; 25:253–261.
38. van Dongen GAMS, Visser GWM, Hooge MNLD, De Vries EG, Perk LR. Immuno-PET: A navigator in monoclonal antibody development and applications. Oncologist. 2007; 12:1379–1389. [PubMed: 18165614]
39. Verel I, Visser GWM, van Dongen GA. The promise of immuno-PET in radioimmunotherapy. J Nucl Med. 2005; 46:164s–171s. [PubMed: 15653665]
40. Keliher EJ, Yoo J, Nahrendorf M, Lewis JS, Marinelli B, Newton A, Pittet MJ, Weissleder R. Zr-89-Labeled Dextran Nanoparticles Allow in Vivo Macrophage Imaging. Bioconjugate Chem. 2011; 22:2383–2389.
41. Abou DS, Thorek DLJ, Ramos NN, Pinkse MWH, Wolterbeek HT, Carlin SD, Beattie BJ, Lewis JS. Zr-89-Labeled Paramagnetic Octreotide-Liposomes for PET MR Imaging of Cancer. Pharm Res. 2013; 30:878–888. [PubMed: 23224977]
42. Rygh CB, Qin SP, Seo JW, Mahakian LM, Zhang H, Adamson R, Chen JQ, Borowsky AD, Cardiff RD, Reed RK, Curry FRE, Ferrara KW. Longitudinal Investigation of Permeability and Distribution of Macromolecules in Mouse Malignant Transformation Using PET. Clin Cancer Res. 2011; 17:550–559. [PubMed: 21106723]
43. Wong AW, Ormsby E, Zhang H, Seo JW, Mahakian LM, Caskey CF, Ferrara KW. A comparison of image contrast with ^{64}Cu-labeled long circulating liposomes and ^{18}F-FDG in a murine model of mammary carcinoma. Am J Nucl Med Mol Imaging. 2013; 3:32–43. [PubMed: 23342299]

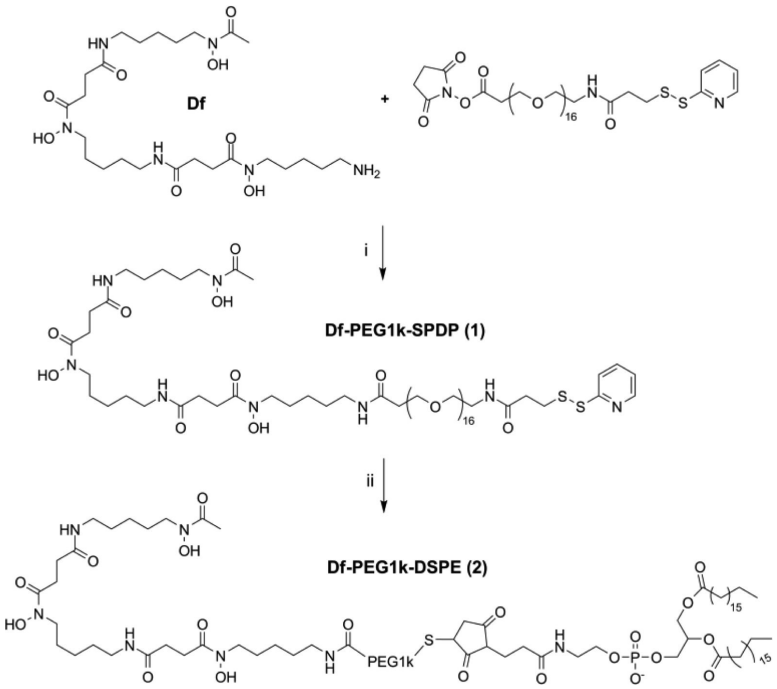

Scheme 1.

i) DIPEA, DMSO, 4 h, ii) DSPE-maleimide, TCEP, H_2O, 4 h.

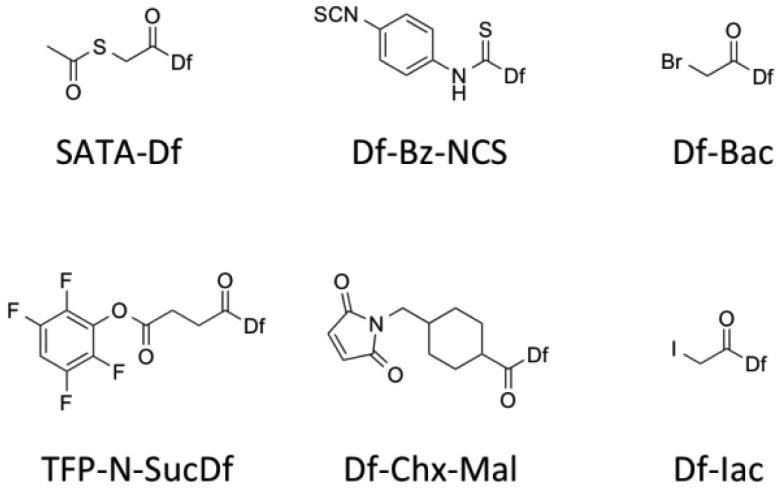

Figure 1.
Bifunctional chelators for ^{89}Zr labeling

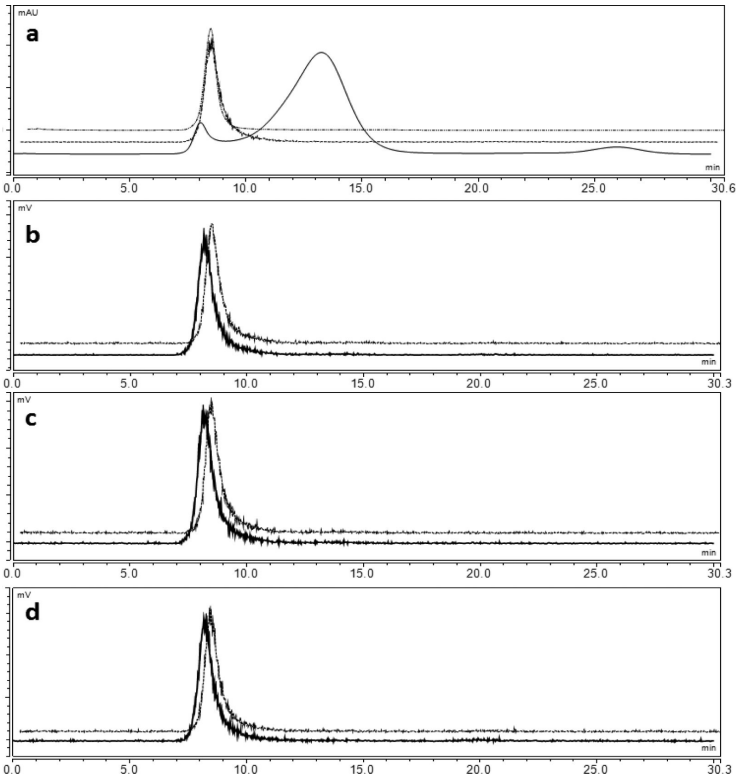

Figure 2.

Size-exclusion chromatograms of ^{89}Zr labeled liposomes. (a) UV absorbance (280 nm) of human serum (solid line), ^{89}Zr-df liposomes only (dotted middle line) and radioactivity chromatogram of ^{89}Zr-df liposomes only (irregular dotted line). Radioactivity chromatograms of (b) ^{89}Zr-df liposomes, (c) ^{89}Zr-df-PEG1k liposomes and (d) ^{89}Zr-df-PEG2k liposomes acquired at 24 (bold front line) and 48 hours (dotted back line) post-incubation with human serum at 37 °C.

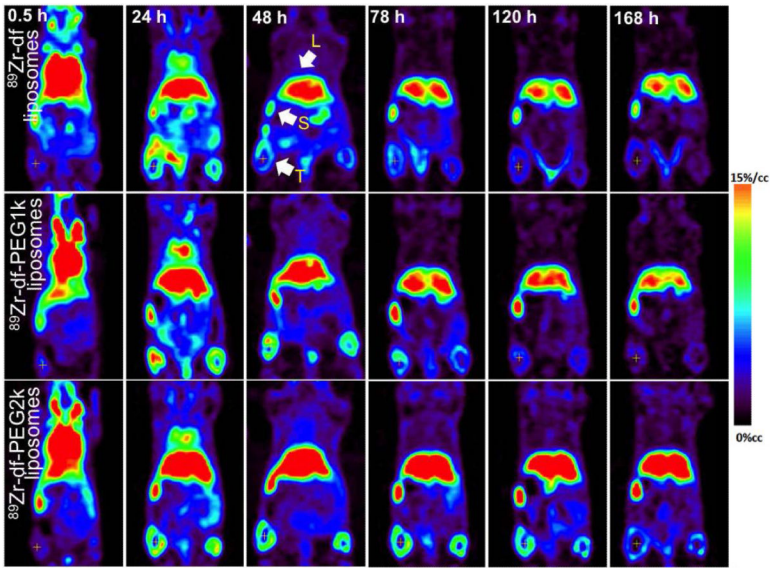

Figure 3.

Time series of small-animal coronal PET images at indicated time points after injection of ^{89}Zr-df liposomes (left), ^{89}Zr-df-PEG1k liposomes (middle), and ^{89}Zr-df-PEG2k liposomes (right). Cross at flank indicates left tumor. Images are decay-corrected and represented at %ID/cc from injected dose. White arrows indicate spleen (S), liver (L) and tumor (T).

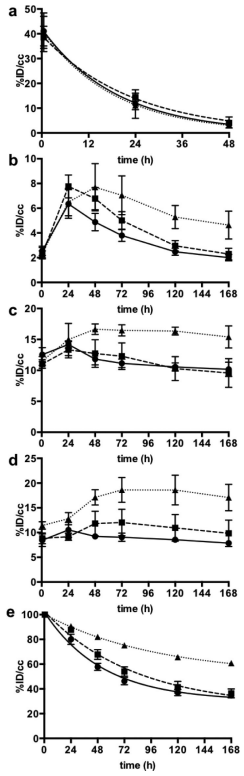

Figure 4.

Timeactivity curves (TAC) obtained from regions-of-interest (ROIs) for (a) blood, (b) tumor, (c) liver, (d) spleen and (e) whole body radioactivity as %ID/cc (solid line: ^{89}Zr-df liposomes, dashed line: ^{89}Zr-df-PEG1k liposomes, dotted line: ^{89}Zr-df-PEG2k liposomes).

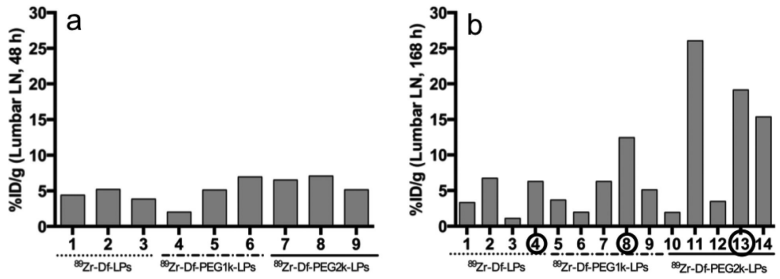

Figure 5.

Radioactivity counts (%ID/g) of lumbar lymph nodes at (a) 48 hours and (b)168 hours. Each given number represents the animal tag number. Lymph nodes from the circled numbers (b) were used for immunohistochemistry (CK8/18, Fig. SI-5 staining).

Table 1

Liposomal formulation and DLS particle sizing

Liposomes (LP)	Lipid components (mol%)				DLS[e] particle sizing (mean ± SD, nm)		
	a	b	c	d	before conjugation	after SEC[f]	after centrifugation
df-LP	55	5	39	1	109 ± 36 (NH_2-LP)	116 ± 15	116 ± 15
df-PEG1k-LP	56	4	39	1	-	118 ± 19	114 ± 15
df-PEG2k-LP	56	4	39	1	119 ± 18 (NH_2-PEG2k-LP)	120 ± 18	120 ± 20

a. HSPC, b. DSPE-PEG2k-OMe, c. cholesterol, d. NH_2-DSPE, df-PEG1k-DSPE, and NH_2-PEG2k-DSPE

[e] dynamic light scattering

[f] size exclusion chromatography

Table 2

In vitro stability of ^{89}Zr-labeled liposomes in 50% serum solution

Time (h)	% radioactivity of total in liposomal peak		
	^{89}Zr-df liposomes	^{89}Zr-df-PEG1k liposomes	^{89}Zr-df-PEG2k liposomes
0	93.5	94.6	93.7
48	92.4	92.2	90.9
Ratio[a]	98.8	97.5	97.0

[a]Ratio of activity at 48 hours normalized by activity at 0 hours * 100

Table 3

Pharmacokinetic parameters from compartmental model

Liposomes	half-life[a] in blood ($t_{1/2}$, h)	VD[b] (mL)	CL[c] (mL/h)
^{89}Zr-df liposomes	13.1 ± 3.27	2.47 ± 0.33	0.085 ± 0.012
^{89}Zr-df-PEG1k liposomes	15.9 ± 1.07	2.62 ± 0.27	0.077 ± 0.008
^{89}Zr-Df-PEG2k liposomes	12.8 ± 0.84	2.53 ± 0.41	0.053 ± 0.008

[a] The half-life was obtained from one-phase exponential decay curve fit ($Y=A\ e^{-k\times t}$).

[b] VD: Volume of distribution.

[c] CL: clearance from whole body. c. The clearance standard deviation was derived by multiplying the average elimination rate with the mouse weight standard deviation

Table 4

Biodistribution of ^{89}Zr-labeled liposomes in selected tissue at 48 and 168 hours

48 hours	^{89}Zr-df liposomes (n = 3)		^{89}Zr-df-PEG1k liposomes (n = 3)		^{89}Zr-df-PEG2k liposomes (n = 3)	
	average	st dev	average	st dev	average	st dev
blood	3.71	0.61	2.70	0.45	3.13	0.33
urine	1.16	0.433	3.61	1.15	1.83	0.84
heart	2.14	0.32	1.82	0.28	2.49	0.58
lungs	2.47	0.38	2.25	0.60	2.95	0.84
liver	14.21	1.88	16.11	1.32	20.93	2.39
spleen	13.31	1.14	20.09	3.02	24.53	1.94
kidneys	6.45	0.30	7.71	0.13	8.54	1.14
muscle	1.08	0.58	1.77	0.95	1.51	0.24
bone	1.51	0.28	2.86	0.37	4.84	0.41
colon	5.10	1.95	2.23	0.38	2.87	0.29
Sm Int[a]	4.49	1.07	6.58	1.37	6.86	0.11
tumor	8.41	0.97	10.46	1.36	13.34	0.83

168 hours	(n = 4)		(n = 5)		(n = 5)	
	average	st dev	average	st dev	average	st dev
blood	0.04	0.02	0.03	0.01	0.05	0.02
urine	0.08	0.01	0.34	0.17	0.49	0.21
heart	1.19	0.30	1.44	0.34	2.41	0.48
lungs	1.19	0.26	1.12	0.17	2.05	0.44
liver	13.91	2.03	13.42	2.42	22.05	2.26
spleen	22.84	3.07	38.41	9.26	65.69	24.35
kidneys	3.67	0.61	3.58	0.65	7.17	1.87
muscle	0.40	0.12	0.41	0.08	0.83	0.45
bone	1.91	0.61	2.77	0.26	3.91	1.16
colon	1.05	0.18	0.88	0.21	1.61	0.40
Sm Int[a]	2.60	0.75	2.40	0.49	4.22	0.60
tumor	3.56	0.99	4.33	1.45	8.05	1.17

Unit is %ID/g.

Statistical analysis by multiple comparisons is attached in SI-6 (Table SI-6-1)

[a]Sm Int: small intestine.